Glycolipid Biomaterials: Solid-State Properties of a Poly(sophorolipid)

Elisa Zini,[†] Massimo Gazzano,[‡] and Mariastella Scandola*,[†]

Department of Chemistry "G. Ciamician", University of Bologna, and National Consortium of Materials Science and Technology (INSTM, UdR Bologna), via Selmi 2, 40126 Bologna, Italy, and ISOF-C.N.R., c/o Department of Chemistry "G. Ciamician", via Selmi 2, 40126 Bologna, Italy

Sabine R. Wallner and Richard A. Gross*

NSF-I/UCRC Center for Biocatalysis and Bioprocessing of Macromolecules, Department of Chemical and Biological Sciences, Polytechnic University, Six Metrotech Center, Brooklyn, New York 11201

Received March 5, 2008; Revised Manuscript Received June 3, 2008

ABSTRACT: Structural complexity inherited from a microbial synthesis of glycolipids was translated into unique poly(sophorolipid) biomaterials. ROMP polymerization of natural diacetylated lactonic sophorolipids gave a high molecular weight polymer with asymmetric bola-amphiphilic repeating units. The poly(sophorolipid) chain alternates C18 oleic-like aliphatic segments (90% cis-configured double bonds) with bulky diacetylated disaccharide moieties. The solid-state properties were investigated by means of TGA, DSC, TMDSC, and variable-temperature X-ray diffraction. The poly(sophorolipid) is a solid at room temperature that undergoes the glass transition at 61 °C and melts at 123 °C. The crystal phase is associated with ordered packing of the aliphatic chain segments. The semicrystalline poly(sophorolipid) also displays a long-range order ($d = 2.44$ nm) involving sophorose groups that is found to persist after crystal phase melting (in high-T diffractograms) with a slightly shortened distance (2.27 nm). Upon annealing at 80 °C the poly(sophorolipid) recrystallizes and concomitantly the disaccharide units space out again at 2.44 nm. An exothermal phenomenon that immediately follows melting and is revealed by TMDSC might be associated with the observed adjustment of sophorose units spacing in the melt. The peculiar structural organization of this novel biomaterial is discussed.

Introduction

Sophorolipids are extracellular glycolipids fermentatively produced by yeast such as *Candida bombicola* from a mixture of carbohydrates and lipids.[1,2] When produced by fermentation of *Candida bombicola* on glucose/oleic acid, sophorolipids are formed as a mixture of at least eight components including lactonic and acidic forms.[1,2] Natural sophorolipids and selected derivatives have shown promise for uses as surfactants, emulsifiers, and therapeutic agents (antibacterial, antifungal, septic shock, anticancer, etc.).[3−5]

The acidic form of sophorolipids produced by yeast is an asymmetrical bola-amphiphile ("bola") constituted by a monounsaturated C_{18} aliphatic chain carrying two differently sized polar groups at the ends (a carboxylic acid at one end and a disaccharide at the other). Fuhrhop and Wang recently reviewed the supramolecular self-assemblies of bolas.[6] Depending on the dimensions and types of polar headgroups and on the number of carbon atoms in the aliphatic spacer, bolas can self-arrange in monolayer lipid membrane vescicles, nanowells, planar monolayers, helical or straight fibers, or in crystals constituted by several packing orders of planar monolayers.[6] Indeed, sophorolipids in the acidic form were found[7] to self-organize into a supramolecular assembly in water at acidic pH to form giant twisted helical ribbons, 5−11 μm wide and several hundred micrometers long. The molecules in the ribbons form a highly ordered layered structure by interdigitated packing. This structure is stabilized both by strong hydrogen bonding between glucose ring hydroxyls and by hydrophobic interactions between parallel arranged aliphatic segments.

The diacetylated lactonic form of sophorolipids, which is most abundant among the mixture of natural sophorolipids, was successfully polymerized via ring-opening metathesis polymerization (ROMP) in yields up to 89%, M_n 103 000 and M_w/M_n 2.0.[8] The resulting poly(sophorolipid)s inherit the structural complexity of natural sophorolipids from which they are produced. Chains consist of sugar rings bearing free and acetylated hydroxyl functionalities, linear aliphatic chains, reactive double bonds, and ester links. Thus, poly(sophorolipid)s have both hydrophilic and hydrophobic characteristics, degradable links along chains will allow their use as bioresorbable biomaterials, hydrolytic degradation will give natural structures, and free hydroxyl groups are available for facile attachment of bioactive groups. Furthermore, sophorolipid fermentative synthesis gives products in high volumetric yields (>300 g/L),[1] lactonic sophorolipids are the primary components of sophorolipids mixtures, and lactonic sophorolipid polymerization occurs with high monomer conversion to high molecular weight polymer. Therefore, poly(sophorolipid) synthesis is relatively straightforward and can readily be up-scaled. Moreover, poly(sophorolipid)s thermal stability and temperature range of thermal transitions (see discussion below) should enable their processing into various material forms such as fibers and porous matrices. Thus, it is evident that poly(sophorolipid)s are an exciting new entry into the existing repertoire of available biomaterials. However, much work remains to elucidate their biological and physical characteristics. This paper is focused on elucidating poly(sophorolipid) solid-state properties.

Experimental Part

Materials. C6, C6′ diacetylated sophorolipids were synthesized by fermentation of *Candida bombicola* using a method described elsewhere.[1] The lactonic fraction of the product mixture was purified by silica gel column chromatography by using a methanol/chloroform mixture as eluent. Column-purified lactonic sophorolipids, hereinafter called lactonic sophorolipids, were used as monomers for ROMP polymerization studies. Ring-opening metathesis polymerization (ROMP) of the lactonic sophorolipid

* Corresponding authors.
† University of Bologna.
‡ ISOF-C.N.R.

10.1021/ma800496f CCC: $40.75
Published on Web 09/25/2008

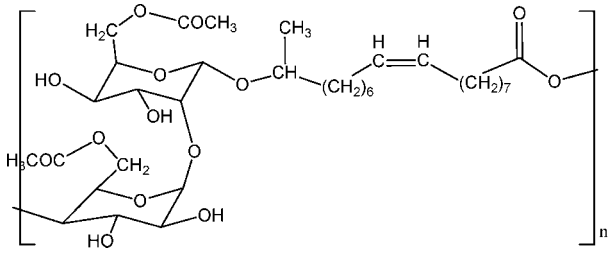

Figure 1. Chemical structure of the poly(sophorolipid).

monomers was conducted in dichloromethane for 5 min at 25 °C using a ruthenium catalyst, as previously reported.[8] The polymer was purified by dissolution in THF and subsequent precipitation in ethanol. The obtained polymer, whose chemical structure is displayed in Figure 1, has a number average molecular weight (M_n) of 37 000 and a polydispersity index (M_w/M_n) of 2.1 (by GPC). Films were obtained by hot pressing the poly(sophorolipid) between Teflon sheets in a Carver press at 150 °C for 1 min. The obtained films (0.2 mm thick) were cooled to room temperature in press using running water.

Characterization Methods. *Structural Analysis.* LC/MS of column-purified materials was performed using an atmospheric pressure chemical ionization (APCI) probe in the positive ion mode with detection in the scan mode (range 170−850 *m/z*). Proton (^{1}H) and carbon (^{13}C) nuclear magnetic resonance (NMR) spectra were recorded in DMSO-d_6 on a Bruker Model DPX300 spectrometer at 300 and 75.13 MHz, respectively. Molecular weights of polyesters were determined by size exclusion chromatography (SEC). The SEC measurements were performed using chloroform as the mobile phase on a Waters HPLC system (Waters Corp., Milford, MA) equipped with a 510 pump, a 717 plus injector, and a 2414 differential refractometer. Further details of the SEC system are described elsewhere.[9]

Solid State Analyses. Thermogravimetric analysis (TGA) was performed with a TA Instruments TGA2950 thermogravimetric analyzer at 10 °C/min from room temperature to 600 °C, both under nitrogen and under air. Differential scanning calorimetry was carried out using a TA Instruments Q100 DSC equipped with the LNCS low-temperature accessory. The temperature scale was calibrated with high purity standards. Thermal scans were performed from −80 to 200 °C, at a heating rate of 20 °C/min in helium atmosphere. Quench cooling was applied between heating scans. The glass transition temperature (T_g) was taken at the midpoint of the stepwise specific heat increment, and the melting temperature (T_m) was taken at the maximum of the endothermal peak. DSC was also used in the temperature modulated mode (TMDSC). For the TMDSC measurements the heating rate was 5 °C/min, whereas oscillation amplitude and oscillation period were 0.5 °C and 40 s, respectively. X-ray diffraction measurements (XRD) were carried out with a PANalytical X'Pert PRO diffractometer equipped with a fast X'Celerator detector. Cu anode was used as X-ray source (K radiation: $\lambda = 0.154$ 18 nm, 40 kV, 40 mA) and 1/4° divergence slit was used to collect the data in the 2θ range of 2°−60°. Real time XRD patterns were collected at different temperatures in the range between room temperature and 180 °C by using an Anton Paar TTK450 heating device. The procedure was the following: a heating scan was run at 20 °C/min and was stopped at selected temperatures, where XRD curves were collected in isothermal mode. Each isothermal data collection lasted about 7 min, then the heating run was resumed.

Results and Discussion

LC/MS analysis of column-purified sophorolipid monomer was performed using an atmospheric pressure chemical ionization (APCI) probe in the positive ion mode with detection in the scan mode (range 170−850 *m/z*). Three major peaks were observed in the LC/MS total ion chromatograph (TIC) corresponding to: (i) two isomers of lactonic diacetate sophorolipids

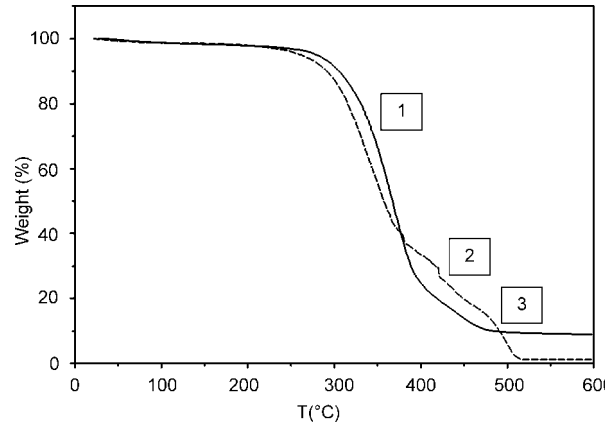

Figure 2. Thermogravimetric curves of the poly(sophorolipid) under nitrogen purge (solid curve) and under air purge (dashed curve); heating rate = 10 °C/min.

with monounsaturated 9-octadecenoic acid distinguished by lipidic moieties with 17- and 18-hydroxy-9-octadecenoic acid, (ii) lactonic diacetate sophorolipid with a saturated lipid moiety. For further details on the LC/MS analysis see ref 8. The ^{1}H NMR spectrum of column purified sophorolipids confirmed they are lactonic with a high degree of acetylation at sophorose 6′- and 6″-positions.[8] Proton NMR analysis of poly(sophorolipid)s is similar to that of the corresponding monomer. The most notable difference is the observation of both cis- and trans-isomers at double bonds (90% cis, 10% trans configuration) whereas the double bond of lactonic diacetate sophorolipids is purely cis.[8]

The above structural analysis studies confirmed that repeat units of poly(sophorolipid) (Figure 1) consist of sophorose disaccharide linked through a glycosidic bond to the penultimate carbon of a monounsatured C_{18} fatty acid and its structure can be assimilated to that of an asymmetrical bola.[6] This specific bola has a lipophilic core, containing one double bond, and two different polar heads, i.e., the ester group at one end and the disaccharide at the other end. The polymer alternates long hydrophobic segments with bulky polar moieties.

Thermal Properties. Figure 2 compares the thermogravimetric curves of the poly(sophorolipid) carried out in air (dashed curve) and in nitrogen (solid curve). Three decomposition events can be identified and are indicated as steps 1, 2, and 3 in Figure 2. Prior to such clear weight loss steps, in the range from room temperature to 150 °C, the poly(sophorolipid) loses about 1.6% of its initial weight both in air and in N_2. This feature is attributed to evaporation of water absorbed by polar segments of the macromolecule. The decomposition behavior at temperatures above 200 °C clearly depends on the purging gas. In nitrogen, the polymer shows two decomposition steps, the main one (step 1) at $T_{max} = 370$ °C and the other (step 2) at 446 °C, with a solid residue at 600 °C of 9%. The thermogravimetric curve under air purge shows a main degradation (step 1, $T_{max} = 342$ °C) about 30 °C below that observed under nitrogen purge, indicating a decrease in thermal stability of the polymer in air. A second weight loss (step 2) occurs in air in the same temperature range as in nitrogen. In air, an additional third step (step 3) results from combustion of compounds that do not degrade under N_2. As a consequence, the solid residue under air purge is lower (2%) compared to that in N_2 (9%).

It is known that cellulose, like most polysaccharides, when subjected to TGA analysis, shows thermal degradation around 350 °C,[10] where cleavage of glycosidic bonds occurs and volatile compounds such as CO, CO_2, etc. are released.[11] On the other hand, the decomposition of a typical polyolefin, i.e., polyethylene, is known to occur above 400 °C, a temperature that

Table 1. Calorimetric Results on Poly(sophorolipid) (First DSC Heating Scan)

sample	T_g (°C)	ΔC_p (J/(g deg))	T_m (°C)	ΔH_m (J/g)	ΔH_{exo} (J/g)
powder[a]	n.d.[f]	n.d.	122	n.d.	n.d.
dried powder[b]	n.d.	n.d.	123	23.8	13.8
film[c]	60	0.41	—	—	—
annealed film[d]	66	0.24	112/123[e]	19.5	1.5

[a] Powder after precipitation from ethanol. [b] Same as (a) dried 48 h on P_2O_5 under reduced pressure. [c] Hot-pressed film dried 48 h on P_2O_5 under reduced pressure. [d] Same as (c) annealed at 80 °C for 48 h. [e] Peak temperatures of multiple endotherm. [f] n.d.= not determined.

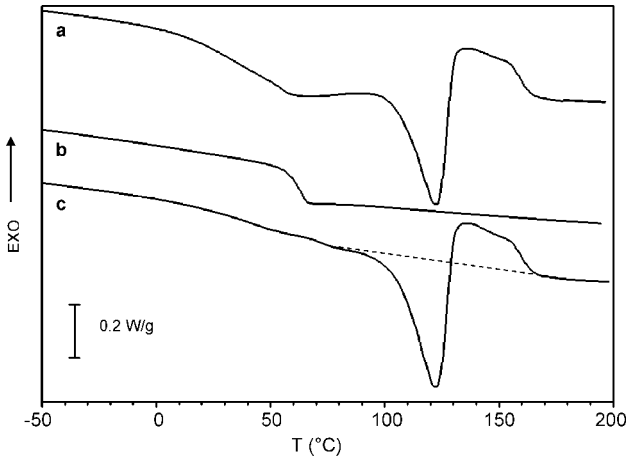

Figure 3. DSC curves of poly(sophorolipid): (a) first scan; (b) second scan after melt quenching; (c) first scan of a predried sample.

slightly decreases in the presence of unsaturations.[12] Also poly(ω-pentadecalactone), a long-chain aliphatic polyester, has been reported to show a TGA behavior very similar to that of polyethylene.[13] Hence, taking into account the structure of the poly(sophorolipid) (Figure 1), step 2 in Figure 2 can be tentatively attributed to thermal degradation of fatty acid segments, whereas step 1, centered around 350 °C, may be associated with degradation of the disaccharide moieties. It is worth noting that the weight loss of step 1 is larger than that of step 2 in both purging conditions (N_2 and air). The ratio between the step intensities roughly corresponds to the calculated weight ratio of aliphatic segments to sophorose groups in the repeating unit (34 to 66 wt %), supporting the above attribution.

Poly(sophorolipid) thermal behavior was also investigated by calorimetric methods. Calorimetric data are collected in Table 1. Figure 3 shows DSC heating curves (first scan, curve a, and second scan after quenching, curve b) of the sample in powder form, as obtained after purification (precipitation in ethanol). Curve a shows a broad endotherm beginning around room temperature (RT), followed by an endo/exothermal complex event. The second scan after melt quenching shows only a clear glass transition at $T_g = 61$ °C. No additional thermal events appear in curve b up to 200 °C. The poly(sophorolipid) sample showed a 2% weight loss after two thermal scans, a value comparable to that observed by TGA analysis between RT and 150 °C (1.6%), attributed to evaporation of absorbed water.

Figure 3 also displays the first scan (curve c) of a poly(sophorolipid) powder sample dried (2 days under reduced pressure over P_2O_5) prior to DSC measurement. The DSC trace shows a neat endotherm ($T_m = 123$ °C), that very abruptly evolves into an exotherm (the baseline is drawn to highlight the two close phenomena). It is worth noting that no further thermal events were observed in DSC heating scans (not shown) run up to 300 °C, i.e., where thermal degradation starts. After the first scan (curve c) followed quench cooling, the predried sample was rerun and a DSC curve (not shown) identical to curve b discussed above was obtained. The only difference, as expected, was the absence in this case of any weight loss at the end of the second run.

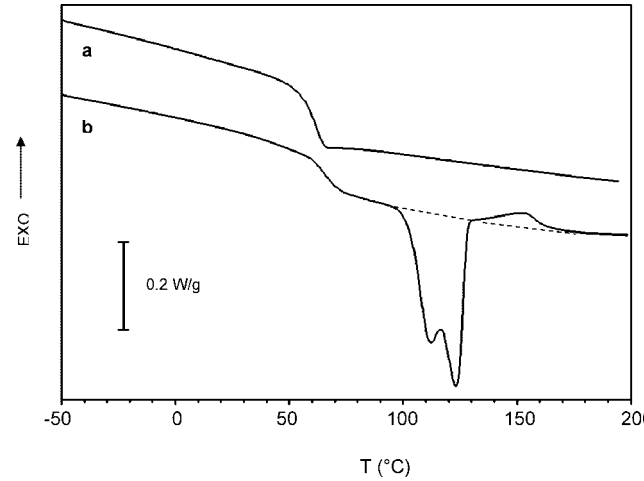

Figure 4. DSC curves of hot-pressed poly(sophorolipid) film (first scan): (a) pre- dried and RT conditioned film; (b) annealed (80 °C for 48 h) and predried film.

The poly(sophorolipid) was hot pressed into a film (see Experimental Part) that, after drying at RT for 2 days under reduced pressure, was analyzed by DSC (Figure 4, curve a). The only feature in the calorimetric curve of the film sample is an intense glass transition. However, if the film is annealed for 48 h in an oven at 80 °C, the first DSC heating scan (curve b in Figure 4) shows, in addition to the glass transition, a multiple endotherm followed by a small exotherm. The temperature range of such endo/exothermal events is the same as that observed in Figure 3 for the dried as-purified powder (curve c). The results in Figure 4 indicate that, by annealing the hot-pressed amorphous film above T_g, the poly(sophorolipid) develops a crystal phase, as confirmed by the decrease of the specific heat increment at the glass transition and by the slight increment of T_g of the annealed sample compared with the melt processed film (Table 1).

In order to investigate the high-temperature exothermal phenomenon that immediately follows the melting endotherm in both Figures 3 and 4, temperature-modulated DSC (TMDSC) was used.[14−17] In the presence of a temperature modulation, the total heat flow (T) is decomposed into two contributions: (i) the reversing heat flow (R) that follows the temperature modulation and is associated with the reversing heat capacity change, and (ii) the nonreversing heat flow (NR) that is mainly affected by the process kinetics.[18] Figure 5 shows TMDSC traces of the dried powdery poly(sophorolipid), whose conventional DSC curve has been discussed above (curve c of Figure 3). The TMDSC results are summarized in Table 2. Taking into account the different heating rates applied (5 °C/min in TMDSC vs 20 °C/min in DSC), the total TMDSC curve closely resembles that obtained for the same poly(sophorolipid) sample by the DSC technique (compare curve T in Figure 5 with curve c in Figure 3). Interestingly, TMDSC allows separation of overlapping endo/exothermal phenomena that occur in the poly(sophorolipid) in the range 80−150 °C (compare curves R and NR). Worth noting is that the nonreversible exotherm in curve NR starts when the endotherm in the reversible curve (R) has not even reached its peak temperature. The peak temperatures of the two processes differ by only 5 deg (Table 2), indicating that the two phenomena are almost concomitant. TMDSC curves (not shown) were also run on hot-pressed poly(sophorolipid) film and no thermal events except the glass transition were found up to 200 °C. This result is consistent with those by DSC in

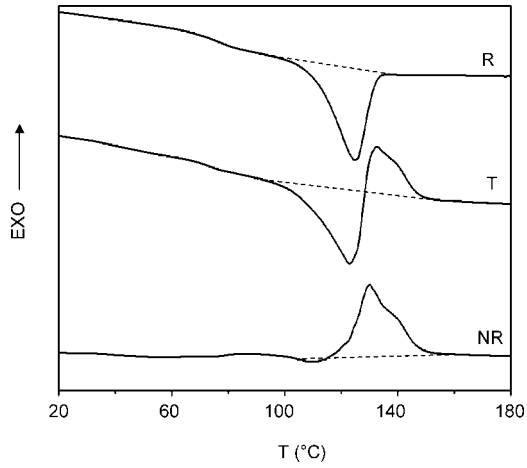

Figure 5. TMDSC curves (first scan) of predried poly(sophorolipid): total heat flow (T), reversible heat flow (R), nonreversible heat flow (NR).

Figures 3 and 4 and it suggests that the exothermal phenomenon appears only when the phase that melts around 120 °C is present.

Structural Characterization. The poly(sophorolipid) was subjected to XRD analysis. Figure 6 shows the XRD patterns at room temperature of the powdery polymer (curve a), of the hot-pressed film (curve b), and of the film annealed at 80 °C for 48 h (curve c), whose respective DSC curves are reported in Figure 3 (curve a) and Figure 4 (curves a and b).

The diffractogram of the polymer powder sample (Figure 6, curve a) shows two small angle reflections at $2\theta = 3.6°$ ($d = 2.44$ nm) and 6.2° and a cluster of broad reflections in the 2θ range from 17° to 25° (maxima at $2\theta = 18.9°$ and $2\theta = 21.6°$) that overlap the amorphous scattering halo.

Earlier work by one of the authors[7] on the non-acetylated sophorolipid molecule in acidic form (i.e., the linear monomer molecule) reported an X-ray diffractogram where a small-angle reflection corresponding to a long period of 2.78 nm was assigned to a highly ordered layered structure generated by the interdigitated sophorolipid bola molecules. In the proposed model, the carboxylic acid group of one molecule faces the sophorose unit of the next molecule, with a 2.78 nm distance between disaccharide layers, while the hydrocarbon chains of the lipidic part of the repeating unit are closely packed in an all-zigzag conformation that bends in correspondence with the cis double bond. Moreover, in this earlier work,[7] the strong crystalline reflections present in the WAXS pattern of the sophorolipid in the d range 0.35−0.5 nm were attributed to packing of hydrocarbon chains into subcells compatible with those generated by the three isomorphic phases (α, β, γ) of oleic acid.[19,20]

The present poly(sophorolipid), as expected, possesses a much poorer crystallinity than the mentioned monomeric linear sophorolipid and reflections at $2\theta = 6.2°$, 18.9°, and 21.6° in the diffractogram (Figure 6, curve a) correspond to distances 1.42, 0.47, and 0.41 nm, respectively. Comparison of the poly(sophorolipid) X-ray pattern with those of the oleic acid polymorphs may shed light into the crystal phase of the polyglycolipid. While several reflections in the 2θ range between 17° and 25° are displayed by all oleic acid isomorphic phases,[19,20] the reflection at $2\theta = 6.2°$ is present only in the pattern of the oleic acid γ phase. Worth noting is that the most intense of the clustered reflections in Figure 6 (curve a) is that at $2\theta = 18.9$, which is also the strongest reflection in the diffractogram of the γ polymorph of oleic acid, associated with the 0.47 nm distance between aliphatic chains. It is therefore inferred that in the poly(sophorolipid) the crystalline reflections in the 2θ range from 17° to 25° and that at $2\theta = 6.2°$ originate from the packing of aliphatic oleic-like segments of the poly(sophorolipid) chain. On the assumption that, as in the γ phase of oleic acid, the C(8)−C(9) = C(10)−C(11) portion of the aliphatic segment is gauche−cis−gauche and that the remaining aliphatic moieties are in the planar zigzag conformation (Figure 7a), the distance between two consecutive sophorose groups along the poly(sophorolipid) chain can be calculated. In the calculation, the disaccharide unit is given the same conformation as that assumed by crystalline sophorose.[21] The obtained distance (2.40 nm) very satisfactorily compares with the experimental long period (2.44 nm) derived from the small angle reflection at $2\theta = 3.6°$ in the diffractogram of the partially crystalline poly(sophorolipid) (curve a, Figure 6). This finding suggests that the observed periodicity regards the sophorose groups segregated at a distance of 2.44 nm by the packed aliphatic segments (see schetch in Figure 7b).

Interestingly, a similar long-range periodicity ($2\theta = 3.9°$, $d = 2.27$ nm) arises from the XRD diffractogram of the melt pressed poly(sophorolipid) film (curve b in Figure 6). In addition to the low-angle reflection, the film that is shown to be completely amorphous by DSC analysis (Figure 4, curve a) also displays (curve b in Figure 6) a broad amorphous phase scattering band centered around $2\theta = 19°$. If, as suggested above, the long-range periodicity in the crystalline poly(sophorolipid) is related to sophorose unit spacing, the observed permanence of a small-angle reflection in the diffractogram of the amorphous sample indicates that the disaccharide units maintain a fixed mutual distance, even when the aliphatic part of the repeating unit assumes disordered conformations. This result suggests the existence of some kind of interaction involving the disaccharide moieties that stabilizes their relative location also in the amorphous film. In the latter case, the periodicity ($d = 2.27$ nm) is slightly shorter than in the semicrystalline poly(sophorolipid).

When the amorphous film is annealed at 80 °C, a crystal phase develops (Figure 6, curve c) with reflections at the same positions as the original poly(sophorolipid) powder (curve a). Worth noting is the shift of the small-angle reflection from $d = 2.27$ nm (amorphous film) to $d = 2.44$ nm (annealed film). The latter value is identical to that of the crystalline powder, supporting the idea that the 2.44 nm periodicity is dictated by the ordered conformation of aliphatic segments connecting sophorose units in polymer chains.

XRD measurements were also carried out at different temperatures on an annealed film sample (the same that, at room temperature, yields curve c in Figure 6). Figure 8 collects XRD curves recorded at 110, 125, 135, and 160 °C, as described in the Experimental Part. The XRD pattern at 110 °C is similar to that recorded at RT (Figure 6, curve c), indicating that no significant changes occur in the crystal phase in the temperature range RT to 110 °C. In the profile recorded at 125 °C, the reflection at $2\theta = 6.2°$ and those in the 2θ interval from 17° to 25° have almost disappeared, showing that the order of the oleic acid segments is lost at this temperature. This result agrees with the presence of a corresponding melting phenomenon (T_m = 122−123 °C, Table 1) in all DSC curves of the semicrystalline polymer. Hence, disordering of the aliphatic chain segments occurs in the poly(sophorolipid) at a temperature close to T_m of low-density polyethylene (LDPE),[22] confirming the above attribution. The XRD diffractograms collected above the melting temperature (Figure 8, $T = 135$ and 160 °C) show, in addition to the expected amorphous scattering band, a reflection at $2\theta = 3.9°$ that becomes broader with increasing temperature. The polysophorolipid quenched from 160 °C down to RT displayed an XRD curve (not shown) identical to that at 160 °C.

Table 2. Temperature-Modulated DSC Results on Poly(sophorolipid)[a]

curve	T_g (°C)	ΔC_p (J/g°)	T_m (°C)	ΔH_m (J/g)	T_{exo} (°C)	ΔH_{exo} (J/g)
total (T)	n.d.[b]	n.d.	123	12.8	133	6.3
reversibile (R)	75	0.26	125	14.9	–	–
nonreversibile (NR)	–	–	–	–	130	11.8

[a] First scan on powder dried 48 h on P_2O_5 under reduced pressure. [b] n.d. = not determined.

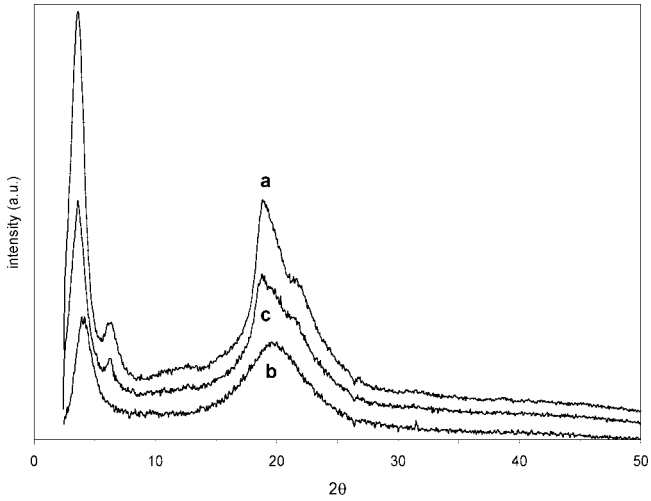

Figure 6. XRD curves of poly(sophorolipid) at room temperature: (a) powder, (b) hot-pressed film, and (c) annealed film (80 °C for 48 h).

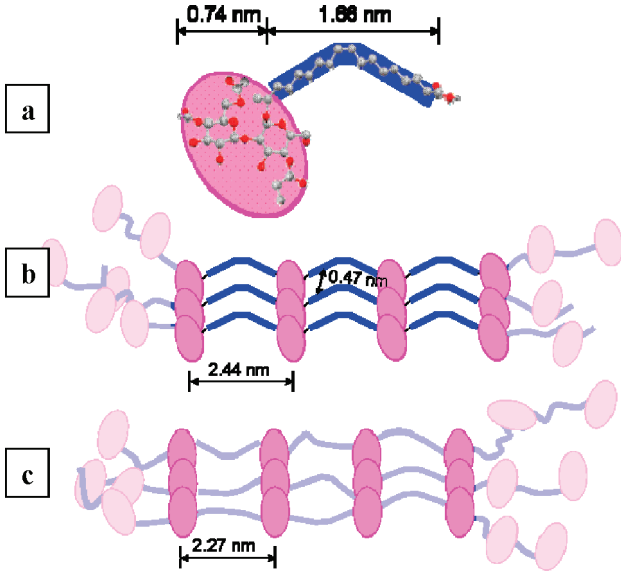

Figure 7. Poly(sophorolipid) packing model: molecular comformation of repeating unit (a) and sketch of a crystalline domain (b). Chain arrangement above the melting temperature (c).

The proposed packing model is sketched in Figure 7. Figure 7b represents the semicrystalline poly(sophorolipid), where the crystalline domains are drawn as closely packed aliphatic segments, with 0.47 nm interchain distance like in oleic acid γ-form, alternated with regularly spaced (2.44 nm) sophorose groups. Above the melting temperature (Figure 7c) the aliphatic segments assume disordered conformations, while the disaccharide units maintain a rather regular though slightly shorter (2.27 nm) spacing distance, that is likely to optimize their mutual interactions. The presently available data do not allow inferring about specific interactions, although the involvement of hydrogen bonding between sugar units might be reasonably suggested.

The TMDSC measurements (Figure 5) have shown an intriguing exothermal phenomenon that partially overlaps melting of the poly(sophorolipid) and that might be somehow connected with the adjustment of the sophorose groups distance above T_m. In order to investigate this point, XRD measurements were conducted isothermally at 135 °C, i.e., within the T range of the TMDSC exotherm, over a period of 20 min. All diffractograms recorded over this time interval were identical to that shown in Figure 8 for the molten polymer (curve T = 135 °C), leading to the conclusion that the heat release generating the exothermal event does not arise from the development of a new crystal phase. Hence this peculiar exothermal process, which occurs in a temperature range where the only structural feature in the XRD diffractogram is a long-range (2.27 nm) periodicity, is tentatively associated with molecular rearrangements that cause the slight change of sophorose group periodicity sketched in Figure 7 and discussed above.

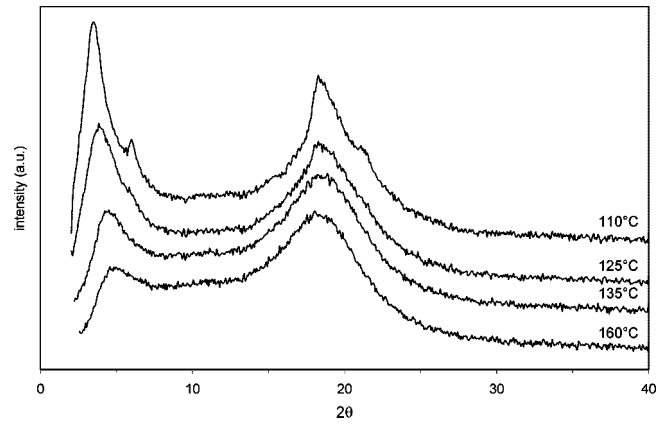

Figure 8. XRD curves of annealed (80 °C for 48 h) poly(sophorolipid) film collected at different temperatures (indicated on curves).

Conclusions

The XRD, DSC, and TMDSC results, altogether, suggest the following picture of poly(sophorolipid) structural organization. The polymer, which is a solid material at room temperature, possesses a crystal phase that melts at 123 °C (close to the LDPE T_m). Poly(sophorolipid) also displays a long-range order, involving sophorose groups, that persists at least up to 160 °C. As the crystal phase starts melting, the increased mobility of the system enables sophorolipid units to reorganize through an exothermal process into a structure with a slightly smaller long period (changing from 2.44 to 2.27 nm). Such a structure that develops quasi-contemporarily to melting is the most stable one in the absence of an ordered packing of the aliphatic stretches. The shorter long period above the melting point is consistent with thermally induced conformational transitions of the aliphatic part of poly(sophorolipid) units and may imply maximization of stabilizing interactions between sophorose moieties. If the amorphous sample is kept at 80 °C (a temperature between T_g and T_m), slow crystallization occurs, involving conformational ordering of the aliphatic segments that once again space out the disaccharide units at 2.44 nm.

The unique structure of poly(sophorolipid)s, which contains free hydroxyl functionalities together with reactive double-bonds, can be exploited to obtain new bioresorbable biomaterials decorated with bioactive moieties. Indeed, we are currently

pursuing this strategy and will report on biological properties of modified poly(sophorolipids)s in a separate report.

Acknowledgment. We thank the Italian Ministry for University and Research (MUR) and the National Science Foundation Industrial/University Cooperative Research Center for Biocatalysis and Bioprocessing of Macromolecules at Polytechnic University for their financial support to this work.

References and Notes

(1) Guilmanov, V.; Ballistreri, A.; Impallomeni, G.; Gross, R. A. *Biotechnol. Bioeng.* **2002**, *77*, 489–494.
(2) Singh, S. K.; Felse, A. P.; Nunez, A.; Foglia, T. A.; Gross, R. A. *J. Org. Chem.* **2003**, *68*, 5466–5477.
(3) Bluth, M. H.; Kandil, E.; Mueller, C. M.; Shah, V.; Lin, Y. Y.; Zhang, H.; Dresner, L.; Lempert, L.; Nowakowski, M.; Gross, R. A.; Schulze, R.; Zenilman, M. E. *Crit. Care Med.* **2006**, *34*, E188.
(4) Shah, V.; Doncel, G. F.; Seyoum, T.; Eaton, K. M.; Zalenskaya, I.; Hagver, R.; Azim, A.; Gross, R. *Antimicrob. Agents Chemother.* **2005**, *49*, 4093–4100.
(5) Van Bogaert, I. N. A.; Saerens, K.; De Muynck, C.; Develter, D.; Soetaert, W.; Vandamme, E. J. *Appl. Microbiol. Biotechnol.* **2007**, *76*, 23–34.
(6) Fuhrhop, J. H.; Wang, T. *Chem. Rev.* **2004**, *104*, 2901–2937.
(7) Zhou, S.; Xu, C.; Wang, J.; Gao, W.; Akhverdiyeva, R.; Shah, V.; Gross, R. *Langmuir* **2004**, *20*, 7926–7932.
(8) Gao, W.; Hagver, R.; Shah, V.; Xie, W.; Gross, R.; Ilker, M. F.; Bell, C.; Burke, K. A.; Coughlin, E. B. *Macromolecules* **2007**, *40*, 145–147.
(9) Sahoo, B.; Bhattacharya, A.; Fu, H.; Gao, W.; Gross, R. A. *Biomacromolecules* **2006**, *7*, 1042–1048.
(10) Zini, E.; Scandola, M.; Gatenholm, P. *Biomacromolecules* **2003**, *4*, 821–827.
(11) Klemm, D.; Philipp, B.; Heinze, T.; Heinze, U.; Wagenknecht, W. In *Comprehensive Cellulose Chemistry*; Wiley-VCH: Weinheim, Germany, 1998; Vol. *1*.
(12) *High Polymers. Part I: Crystalline Olefin Polymers*; Raff, R. A., Doak, K. W., Eds.; John Wiley & Sons: New York, 1965; Vol. *XX*.
(13) Focarete, M. L.; Gazzano, M.; Scandola, M.; Kumar, A.; Gross, R. A. *Macromolecules* **2002**, *35*, 8066–8071.
(14) Liu, T.; Petermann, J. *Polymer* **2001**, *42*, 6453–6461.
(15) Qiu, Z.; Komura, M.; Ikehara, T.; Nishi, T. *Polymer* **2003**, *44*, 7781–7785.
(16) Ribeiro, M.; Grolier, J. P. E. *J. Therm. Anal. Calorim.* **1999**, *57*, 253–263.
(17) Sauer, B. B.; Kampert, W. G.; Blanchard, E. N.; Threefoot, S. A.; Hsiao, B. S. *Polymer* **2000**, *41*, 1099–1108.
(18) Okazaki, I.; Wunderlich, B. *Macromolecules* **1997**, *30*, 1578–1764.
(19) Kaneko, F.; Yamazaki, K.; Kitagawa, K.; Kikyo, T.; Kobayashi, M.; Kitagawa, Y.; Matsuura, Y.; Sato, K.; Suzuki, M. *J. Phys. Chem. B* **1997**, *101*, 1803–1809.
(20) Tandon, P.; Forster, G.; Neubert, R.; Wartewig, S. *J. Mol. Struct.* **2000**, *524*, 201–215.
(21) Ohanessian, P. Q.; Longchambon, F.; Arene, F. *Acta Crystallogr.* **1978**, *B34*, 3666–3671.
(22) Wunderlich, B. Crystal Melting. In *Macromolecular Physics*; Academic Press: New York, 1980; Vol. *III*.

MA800496F